ORIGINAL RESEARCH

Sphingomyelin Synthase 2 Inhibition Ameliorates Cerebral Ischemic Reperfusion Injury Through Reducing the Recruitment of Toll-Like Receptor 4 to Lipid Rafts

Jing Xue, PhD;* Yang Yu, PhD;* Xiangjian Zhang, PhD; Cong Zhang, PhD; Yanan Zhao, MD; Boyan Liu, PhD; Lan Zhang, PhD; Lina Wang, PhD; Rong Chen, PhD; Xuan Gao, PhD; Peng Jiao, MD; Guohua Song, PhD; Xian-Cheng Jiang, PhD; Shucun Qin, PhD

***Background*—**Inflammation is recognized as an important contributor of ischemia/reperfusion (I/R) damage after ischemic stroke. Sphingomyelin synthase 2 (SMS2), the key enzyme for the biosynthesis of sphingomyelin, can function as a critical mediator of inflammation. In the present study, we investigated the role of SMS2 in a mouse model of cerebral I/R.

***Methods and Results*—**Cerebral I/R was induced by 60-minute transient middle cerebral artery occlusion in SMS2 knockout ($SMS2^{-/-}$) mice and wild-type mice. Brain injury was determined by neurological deficits and infarct volume at 24 and 72 hours after transient middle cerebral artery occlusion. Microglia activation and inflammatory factors were detected by immunofluorescence staining, flow cytometry, western blot, and RT-PCR. SMS2 deficiency significantly improved neurological function and minimized infarct volume at 72 hours after transient middle cerebral artery occlusion. The neuroprotective effects of SMS2 deficiency were associated with (1) suppression of microglia activation through Toll-like receptor 4/nuclear factor kappa-light-chain-enhancer of activated B cells pathway and (2) downregulation of the level of galactin-3 and other proinflammatory cytokines. The mechanisms underlying the beneficial effects of SMS2 deficiency may include altering sphingomyelin components in lipid raft fractions, thus impairing the recruitment of Toll-like receptor 4 to lipid rafts and subsequently reducing Toll-like receptor 4/myeloid differentiation factor 2 complex formation on the surface of microglia.

***Conclusions*—**SMS2 deficiency ameliorated inflammatory injury after cerebral I/R in mice, and SMS2 may be a key modulator of Toll-like receptor 4/nuclear factor kappa-light-chain-enhancer of activated B cells activation by disturbing the membrane component homeostasis during cerebral I/R. **(*J Am Heart Assoc*. 2019;8:e012885. DOI: 10.1161/JAHA.119.012885.)**

Key Words: cerebral ischemic reperfusion • inflammation • lipid rafts • sphingomyelin synthase 2 • Toll-like receptor 4

Stroke is one of the leading causes of worldwide death and severe long-term disability in adults.[1] Currently, few clinically efficient medical treatments are available because of the inadequate mechanistic understanding of both ischemic insult and excessive inflammatory response caused by reperfusion.[2] Therefore, it is urgent to develop novel therapeutic agents and explore the underlying mechanisms of ischemic stroke.

A large number of studies have proved that suppression of inflammation is critical to recovery of individuals with ischemic stroke. Toll-like receptors (TLRs), especially TLR4, play a crucial role in postischemic inflammation.[3,4] Activation of the TLR4 signaling pathway is initiated by the binding of its ligands to TLR4, causing TLR4 to relocate to lipid rafts, and then forming TLR4/myeloid differentiation factor 2 (MD2) complex in lipid rafts, leading to activation of nuclear factor

From the Department of Neurology, Second Hospital of Hebei Medical University, Shijiazhuang, China (J.X., X.Z., C.Z., L.Z., L.W., R.C., X.G.); Key Laboratory of Atherosclerosis in Universities of Shandong and Institute of Atherosclerosis, Shandong First Medical University & Shandong Academy of Medical Sciences, Taian, China (Y.Y., Y.Z., B.L., P.J., G.S., S.Q.); Hebei Collaborative Innovation Center for Cardio-cerebrovascular Disease and Hebei Key Laboratory of Vascular Homeostasis, Shijiazhuang, China (J.X., Y.Y., X.Z., C.Z., Y.Z., B.L., L.Z., L.W., R.C., X.G., P.J., G.S., S.Q.); Department of Anatomy and Cell Biology, SUNY Downstate Medical Center, Brooklyn, NY (X.-C.J.).

*Dr Xue and Dr Yu contributed equally to this work.

Correspondence to: Xiangjian Zhang, PhD, Department of Neurology, Second Hospital of Hebei Medical University, 215 Hepingxi Road, Shijiazhuang, Hebei 050000, China. E-mail: zhang6xj@aliyun.com and Shucun Qin, PhD, Key Laboratory of Atherosclerosis in Universities of Shandong and Institute of Atherosclerosis, Shandong First Medical University & Shandong Academy of Medical Sciences, 2 Yingshengdong Road, Taian, Shandong 271000, China. E-mail: shucunqin@hotmail.com

Received April 8, 2019; accepted October 16, 2019.

Clinical Perspective

What Is New?

- The study demonstrated that sphingomyelin synthase 2 deficiency exerted an anti-inflammatory effect after cerebral ischemic reperfusion by impairing Toll-like receptor 4 recruitment to lipid rafts and inhibiting its downstream signal transduction.

What Are the Clinical Implications?

- These findings may shed light on a therapeutic design focusing on the disturbance of membrane component homeostasis to subsequently restrict the inflammatory signaling pathways.

kappa-light-chain-enhancer of activated B cells (NF-κB) and overproduction of proinflammatory cytokines.[5] Lipid rafts, enriched in sphingolipid and cholesterol, are defined as a dynamically formed membrane microdomain.[6] It has been recently reported that formation of lipid rafts is essential for initiation of TLR4 signal transduction, by providing a favorable environment for ligand-receptor association.[7] Moreover, alterations in lipid rafts homeostasis are characteristic of several neurological diseases.[8] Therefore, identification of potential substance that could modulate the homeostasis of lipid rafts to directly inhibit the TLR4 signaling pathway may provide a feasible therapeutic strategy for ameliorating cerebral ischemia/reperfusion (I/R) injury-induced inflammation.

Sphingomyelin synthase (SMS) is a rate-limiting enzyme of sphingomyelin, which is one of the major constituents of lipid rafts.[9] Two isoforms of SMS have been found in mammalian species: SMS1 and SMS2. SMS1 is primarily located in the trans-Golgi apparatus, whereas SMS2 is located in plasma membranes. SMS2 is particularly important for sphingomyelin production in the central nervous system, given that SMS2, rather than SMS1, is highly expressed in brain cells.[10] SMS2 deficiency–induced reduction of sphingomyelin in plasma membrane could disrupt the formation of functional lipid rafts that serve as a platform for initiation of certain signaling cascades.[11] Importantly, SMS2 deficiency exerts anti-inflammatory effects by reducing the abundance of the TLR4/MD2 complex on the surface of macrophages after LPS stimulation.[11] However, the role of SMS2 deficiency in postischemic inflammation remains unclear.

Based on the documented observations above, we hypothesized that SMS2 deficiency might suppress the inflammation induced by cerebral I/R through dampening the TLR4-mediated pathway. In the present study, using a mouse model of cerebral I/R, we evaluated the impacts of SMS2 deficiency on cerebral I/R and investigated the underlying mechanisms.

Materials and Methods

Data Availability

The data that support the findings of this study are available from the corresponding author upon reasonable request.

Experimental Animals

SMS2 knockout ($SMS2^{-/-}$) mice were established as previously reported.[11] The resulting heterozygous mice were crossed, and $SMS2^{-/-}$ mice were obtained. A total of 268 mice were used, and the mice ($SMS2^{-/-}$ and wild type [WT]) used in this experiment were littermates. Animals were housed in a humidity controlled room on a 12-hour light/dark cycle at 22°C with free access to food and water. Adult male mice (8–10 weeks) were used for experiments. All experimental procedures were approved by the committee of experimental animals of Hebei Medical University (Shijiazhuang, China) and conducted in accord with the National Institutes of Health guidelines. Animals were assigned randomly using a random number table. All assessments were conducted by investigators who were blinded to experimental group assignment.

Transient Cerebral Ischemia by Middle Cerebral Artery Occlusion

Mice were anesthetized with 1% pentobarbital (100 mg/kg, IP). Transient cerebral ischemia was induced by the intraluminal filament technique as previously performed.[12] The monofilament was withdrawn after 60 minutes to restore blood flow. To ensure successful occlusion of the artery, a laser Doppler flowmeter (Moor Instruments Ltd, Axminster, UK) was utilized to monitor regional cerebral blood flow (CBF). The baseline of regional CBF was obtained before, during middle cerebral artery occlusion, and after reperfusion, and the middle cerebral artery was occluded with a criterion of <25% of baseline blood flow remaining after middle cerebral artery occlusion.

Investigation of Intracranial Vasculature

To exclude the effects of cerebral vessel anomalies on the outcome of cerebral ischemia, we investigated the vascular anatomy of the circle of Willis in both WT and $SMS2^{-/-}$ mice. After transcardial perfusion with 5 mL of normal saline and 4% PFA, carbon black suspended in 20% gelatin was perfused.[13] Whole brains were carefully removed and then placed in 4% PFA overnight. The circle of Willis and posterior communicating arteries in both hemispheres were examined.

2-Dimensional Laser Speckle Imaging Techniques

To monitor cortical blood flow of WT and $SMS2^{-/-}$ mice, laser speckle perfusion images were obtained before middle

cerebral artery occlusion, during ischemia, and after reperfusion. CBF is expressed as a percentage of pre-tMCAO (transient middle cerebral artery occlusion) baselines.

Behavioral Testing

1. Neurological score: A 5-point neurological score was performed at 24 and 72 hours after reperfusion before anesthesia by a blinded investigator.[14] Briefly, "0" stands for no deficits; "1" stands for difficulty in fully extending the contralateral forelimb; "2" stands for unable to extend the contralateral forelimb; "3" stands for mild circling to the contralateral side; "4" stands for severe circling movements; and "5" stands for falling to the contralateral side.
2. 28-point neuroscore: The 28-point neuroscore was used to assess sensorimotor function as previously described.[15] Scores for the following 11 tests are summed to give a maximum total score of 28 points: (1) circling (maximum score 4); (2) motility (maximum score 3); (3) general condition (maximum score 3); (4) righting reflex when placed on back (maximum score 1); (5) paw placement of each paw onto a table top (maximum score 4); (6) behavior on a horizontal bar (maximum score 3); (7) behavior on an inclined platform (maximum score 3); (8) grip strength (maximum score 2); (9) contralateral reflex (maximum score 1); (10) contralateral rotation (maximum 2); and (11) visual forepaw reaching (maximum score 2). Baseline evaluation of these tests was performed 24 hours before tMCAO.
3. Corner test: The corner test was used to evaluate sensorimotor asymmetry, according to the previous description.[16] Mice were placed facing the corner, which is composed by 2 boards placed closely together with an angle of 30 degrees. When mice approached the corner, both sides of the vibrissae were simultaneously stimulated, leading the mice to rear forward and upward, then turn 180 degrees to face the open end. Intact mice will turn to the right or left randomly, whereas mice after tMCAO will preferentially turn around in the ipsilateral direction. Baseline data are conducted to reduce the variability as well as identifying any preferential side. The test was repeated 10 times, with at least 30 seconds between trials, and the numbers of right turns were calculated. Only turning movements involving a rearing movement were included.
4. Gait analysis: The gait of WT and SMS2$^{-/-}$ mice was analyzed using the TreadScan instruments (Columbus Instruments, Columbus, OH), according to the manufacturer's instructions and a reported description.[17] Briefly, the video treadmill system is made up of a treadmill belt with a mirror mounted below. A high-speed digital video camera was mounted underneath the treadmill to record the movements of all 4 paws at a rate of 100 frames/sec for 20 seconds. A background image was taken before each test day. Each mouse was acclimatized in the setup and trained 3 days before tMCAO and at 24 hours, 72 hours after tMCAO at a speed of 8 cm/s or the maximum speed at which mice were able to maintain optimally coordinated locomotion. Segments of at least 6 consecutive step cycles were selected for automated gait analysis. Automated footprint analysis of gait was conducted, and average values for each limb were used for statistical analysis of all available parameters of gait by CleverSys TreadScan software (CleverSys, Inc., Reston, VA).

Measurement of Infarction Volume

Infarction volume was evaluated at 24 and 72 hours after reperfusion. Mice were euthanized by decapitation, and brains were removed and cut into 5 coronal sections (2-mm thickness) with a brain matrix, which were stained with 2% TTC. Infarct volume was determined as: %HLV={[total infarct volume−(volume of intact ipsilateral hemisphere−volume of intact contralateral hemisphere)]/contralateral hemisphere volume}.[18]

Western Blot

Cortical tissues were collected from the peri-infarct area at 24 and 72 hours after cerebral I/R and the corresponding area in sham mice. Protein from cortical tissues was extracted as previously described.[19] Various primary antibodies were used, including galectin-3 (Gal-3; 1:1000; Abcam Cat#ab53082 RRID:AB_880159; Abcam, Cambridge, MA), NF-κB p65 (1:1000; Abcam Cat#ab31481 RRID:AB_2300947), TLR4 (1:500; Abcam Cat#ab13556 RRID:AB_300457), flotillin-1 (1:1000; Abcam Cat#ab41927 RRID:AB_941621), GAPDH (1:500; Abcam Cat#ab9485 RRID:AB_307275), β-actin (1:3000; Sigma-Aldrich Cat#A2228 RRID:AB_476697; Sigma-Aldrich, St. Louis, MO), and H3 (1:500; Abcam Cat#ab8898 RRID:AB_306848).

Quantitative Real-Time PCR

Brain tissues were collected from the peri-infarct area at 24 and 72 hours after cerebral I/R and the corresponding area in sham mice. Total RNA was extracted and quantitative real-time RT-PCR was performed as previously described.[19] The primer sequences were as follows: interleukin-1 beta (forward, 5′-ACTGTTTCTAATGCCTTCCC-3′; reverse, 5′-ATGGTTTCTTGTGACCCTGA-3′), inducible nitric oxide synthase (iNOS; forward, 5′-TGGTGGTGACAAGCACATTT-3′; reverse, 5′-AAGGCCAAACACAGCATACC-3′), arginase 1 (Arg-1; forward, 5′-TCATGGAAGTGAACCCAACTCTTG-3′; reverse, 5′-TCAGTCCCTGGCTTATGG

TTACC-3′), Gal-3 (forward, 5′-TTTCAGGAGAGGGAATGATGTTG-3′; reverse, 5′-CACAATGACTCTCCTGTTGTTCTCA-3′), and GAPDH (forward, 5′-TGACGTGCCGCCTGGAGAAA-3′; reverse, 5′-AGTGTAGCCCAAGATGCCCTTCAG-3′).

Immunohistochemical Staining

Deeply anesthetized mice were perfused intracardially with cold PBS and followed by 4% PFA at 24 and 72 hours after cerebral I/R. Immunohistochemical staining of frozen coronal brain slices were performed as we previously described.[20] Frozen coronal brain slices (30 μm) were permeabilized with 0.3% Triton X-100 for 30 minutes. Slices were blocked with 10% normal donkey serum for 30 minutes and then incubated in the primary antibodies overnight at 4°C: mouse anti–ionized calcium binding adaptor molecule 1 (Iba-1; 1:500; Abcam Cat#ab5076 RRID:AB_2224402) to identify microglia and anti-Gal-3 (1:200; Abcam Cat#ab53082 RRID:AB_880159). After slices were washed with PBS on the second day, they were incubated in antirabbit FITC-conjugated secondary antibody (1:600; Zhongshan Bio-Tech Co., Ltd., Zhongshan, China) or antigoat TRITC-conjugated secondary antibody (1:200; Zhongshan Bio-Tech Co., Ltd.) for 2 hours. To identify the nucleus, brain slices were counterstained with Hoechst (10 μg/mL) for 15 minutes. Images were acquired on a ×40 Laser Scanning Confocal Microscope (Carl Zeiss, Jena, Germany). The number of positively stained cells was counted on the cortex in the peri-infarct area and the corresponding area in the contralateral cortex at the caudoputamen level. The numbers of positive cells within 5 fields of each section are expressed as an average value.

Preparation of Single-Cell Suspension and Flow Cytometry

At 72 hours after cerebral I/R, mice were anesthetized and received transcranial perfusion with HBSS. Brain tissues from the peri-infarct area were collected. A single-cell suspension was prepared as described before.[21,22] For flow cytometry analysis, cells were stained on ice for 20 minutes with antimouse TLR4 Alexa Fluor 488 (1:50; eBioscience Cat#53-9041 RRID:AB_469944; eBioscience, Inc., San Diego, CA), antimouse CD11b PE (1:150; eBioscience Cat#12-0112 RRID:AB_465546), antimouse CD45 APC (1:150; eBioscience Cat#17-0451 RRID:AB_469393), antimouse TLR4/MD2 complex PE (1:40; eBioscience Cat#12-9924 RRID:AB_466264), antimouse CD11b Alexa Fluor 488 (1:100; eBioscience Cat#53-0112 RRID:AB_469900), or antimouse CD45 APC (1:150; eBioscience Cat#17-0451 RRID:AB_469393) and then washed with HBSS. Data were collected and analyzed on a flow cytometer (BD FACSCalibur; BD Biosciences, San Jose, CA).

Lipid Raft Isolation

Brain tissues from the peri-infarct area were collected at 24 and 72 hours after cerebral I/R. Lipid raft isolation was performed as previously described.[23] Lipid fractions were identified by the presence of flotillin-1, a lipid raft marker.[24]

Sphingomyelin Quantification by Liquid Chromatography/Tandem Mass Spectrometry

Brain tissue was homogenized and sphingomyelin was extracted using an alkaline MTBE method as previously described.[25,26] Liquid chromatography/electrospray ionization/tandem mass spectrometry was performed using a Shimadzu LC-20 AD binary pump system coupled to a SIL-20AC autoinjector and DGU20A3 degasser interfaced with an ABI 4000 QTrap mass spectrometer (Applied Biosystems Division, Life Technologies, Carlsbad, CA) equipped with an electrospray ionization source. Chromatographic separations were carried out on a Waters Symmetry C18 column (3.5 μm, 2.1 mm i.d.×100 mm) with a Waters C18 guard column (3.5 μm, 2.1 mm i.d.×10 mm; Waters Corporation, Milford, MA). The mobile phase consisted of 2 mmol/L of ammonium and 0.2% formic acid in 50% methanol aqueous solution (A) and 100% methanol (B). The gradient elution program was as follows: 0 to 3 minutes, 50% of B; 3 to 10 minutes, 50% to 98% of B; and 10 to 25 minutes, 98% of B. The injection volume was 10 μL, and the flow rate was 0.4 mL/min; the oven temperature was maintained at 40°C. The mass spectrometer was operated in the positive ion mode with an ionspray voltage of 5500 V at 550°C and supplied by auxiliary gas at 20 psi. Nebulizer gas was set at 20 psi, curtain gas at 10 psi, and collision gas at medium. Measurements correspond to the intensity of each species divided by the intensity of the internal standard sphingomyelin d18:1/12:0 (Avanti Polar Lipids, Alabaster, AL).

Statistical Analysis

Quantitative data were processed by SPSS software (version 13.0; SPSS, Inc., Chicago, IL) and are represented as mean ±SEM if normally distributed, otherwise as median and interquartile range. The in vivo experiments were repeated 3 times, and the results of in vitro experiments are representative of at least 3 independent experiments. Differences between 2 groups were assessed by the 2-tailed Student *t* test. For multiple comparisons, differences were assessed by 1-way ANOVA followed by Student–Newman–Keuls tests. For data that were not normally distributed in the analyses of neurological scores, RT-PCR, and western blot, nonparametric tests were conducted. The Mann–Whitney *U* test was used for comparisons between 2 groups, and the Kruskal–Wallis test was used for multiple comparisons among ≥3 groups. Difference were considered significant when $P<0.05$.

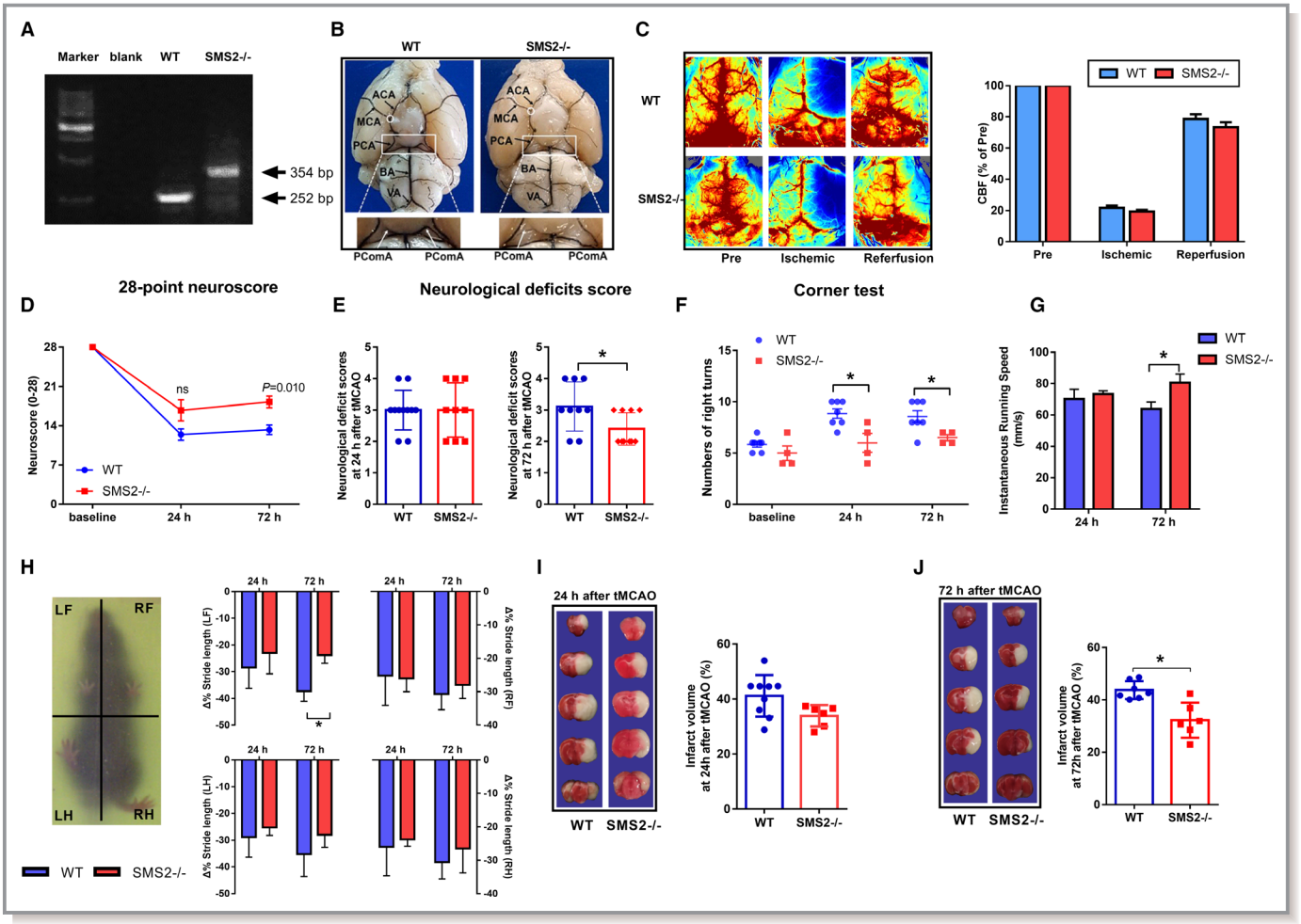

Figure 1. SMS2 deficiency protected mice against cerebral ischemic reperfusion injury after tMCAO. **A**, Genotype determination of SMS2-deficient mice. Genotypes of SMS2 were determined by PCR. WT mice had a 252-bp (base pair) PCR product, and SMS2$^{-/-}$ mice had a 354-bp PCR product. **B**, Brain vasculature of WT and SMS2$^{-/-}$ mice perfused transcardially with carbon lampblack in 20% gelatin ddH_2O (n=6). **C**, Representative and quantification images of CBF before tMCAO, during tMCAO and at 10 minutes after reperfusion for each group using 2-dimensional laser speckle imaging (WT=4, SMS2$^{-/-}$=5, respectively). **D**, Twenty-eight-point neuroscore of WT (n=7) and SMS2$^{-/-}$ mice (n=4) before and at 24 and 72 hours after cerebral ischemic reperfusion (*P<0.05 vs WT group, Mann–Whitney U test). **E**, Neurological deficits of WT (n=11) and SMS2$^{-/-}$ mice (n=9) at 24 and 72 hours after cerebral ischemic reperfusion (*P<0.05 vs WT group, Mann–Whitney U test). **F**, Corner test of WT (n=7) and SMS2$^{-/-}$ mice (n=4) before and at 24 and 72 hours after cerebral ischemic reperfusion (*P<0.05 vs WT group, Mann–Whitney U test). **G**, Instantaneous running speed of WT (n=7) and SMS2$^{-/-}$ mice (n=4) at 24 and 72 hours after cerebral ischemic reperfusion (*P<0.05 vs WT group, Student t test). **H**, Normalization of stride length for all paws of WT (n=7) and SMS2$^{-/-}$ mice (n=4) at 24 and 72 hours after cerebral ischemic reperfusion. Data are presented as mean±SEM percentage changes (Δ%) between pre-tMCAO and post-tMCAO. LF indicates left front paw; LH, left hind paw; RF, right front paw; RH, right hind paw (*P<0.05 vs WT group, Mann–Whitney U test). **I**, Representative images and quantification of TTC-staining brain slices of WT (n=9) and SMS2$^{-/-}$ mice (n=6) at 24 hours after cerebral ischemic reperfusion. **J**, Representative images and quantification of TTC-staining brain slices of WT (n=9) and SMS2$^{-/-}$ mice (n=6) at 72 hours after cerebral ischemic reperfusion (*P<0.05 vs WT group, 2-tailed Student t test). Data are mean±SEM. CBF indicates cerebral blood flow; SMS2, sphingomyelin synthase 2; tMCAO, transient middle cerebral artery occlusion; WT, wild type.

Results

SMS2 Deficiency Ameliorated Neurological Deficits and Infarct Volume After Cerebral I/R

The genomic DNA from mice tail tip was isolated to identify the genotype of SMS2$^{-/-}$ by PCR. The single band of 252 base pairs and a single band of 354 base pairs PCR products indicated the WT and SMS2$^{-/-}$ homozygous, respectively (Figure 1A).

We evaluated vascular anatomy of the circle of Willis, given that the genetic modification may cause the anatomical variation of posterior communicating artery and influence the outcome of cerebral ischemia. The results showed there was no significant difference between WT and SMS2$^{-/-}$ mice in the patency of the posterior communicating artery that would account for the observed differences in cerebral I/R injury (Figure 1B). Regional CBF was monitored before, during, and

after tMCAO by laser speckle 2-dimensional imaging (Figure 1C). There was no statistical difference in CBF before, during, and after tMCAO between the WT and SMS2$^{-/-}$ mice, verifying that all animals were subjected to the same extent of cerebral ischemia and achieved the same degree of reperfusion.

To investigate the potential role of SMS2 deficiency in animal models of cerebral I/R, we determined the degree of ischemic injury by measuring neurological deficit score, 28-point neuroscore, corner tests, and gait analysis, all of which are reliable tests for the middle cerebral artery occlusion model.[15,27]

The 28-point neuroscore showed general neurological deficit at 24 and 72 hours after tMCAO compared with baseline. Importantly, WT mice showed significant impairment compared with SMS2$^{-/-}$ mice at 72 hours after tMCAO (Figure 1D; tMCAO: WT group versus SMS2$^{-/-}$ group: 14 [12, 15] versus 18 [16.5, 20.25]; P=0.010).

The results of neurological deficits scores showed that there was significant improvement in neurological deficits in SMS2$^{-/-}$ mice compared with WT mice at 72 hours after tMCAO, which indicated restoration of neurological functions (Figure 1E; 72 hours after tMCAO: WT group versus SMS2$^{-/-}$ group: 3 [2.5, 4] versus 2 [2, 3]; P=0.02). However, there was no statistical significance between WT and SMS2$^{-/-}$ mice at 24 hours after tMCAO (Figure 1E, 24 hours after tMCAO: WT group versus SMS2$^{-/-}$ group: 3 [3, 3] versus 3 [2, 4]; P=1.00).

In the corner test, mice subjected to tMCAO showed increased numbers of right turns compared with baseline. Moreover, SMS2$^{-/-}$ mice exhibited less numbers of right turns compared with WT mice at both 24 and 72 hours after tMCAO (Figure 1F; tMCAO: WT group versus SMS2$^{-/-}$ group: 9 [8, 10] versus 6 [4.25, 7.75] [24 hours], 8 [8, 10] versus 6.5 [6, 7] [72 hours]; P=0.026 and 0.032, respectively).

We next sought to improve the accuracy of the functional analysis by means of gait analysis using the TreadScan system (CleverSys, Inc.). Temporal and spatial parameters were affected by ischemia. Instantaneous running speed was decreased and the stride length for all 4 paws was increased at 24 and 72 hours after tMCAO, in comparison with their control values before tMCAO in both the WT and SMS2$^{-/-}$ groups. The results showed that stride length of both contralateral and ipsilateral sides was increased, which could be explained by a strong intercoordination of limbs in quadrupedal gait. Importantly, some improvement of selected gait parameters was observed in SMS2$^{-/-}$ mice at 72 hours after tMCAO. Instantaneous running speed of SMS2$^{-/-}$ mice was improved in comparison with WT mice (Figure 1G; P=0.045). The improvement of stride length for all 4 paws in SMS2$^{-/-}$ group did not attain statistical significance in comparison with the WT group, with the exception of the left front paw at 72 hours after tMCAO (Figure 1H; tMCAO: WT group versus SMS2$^{-/-}$ group: -37 [-50, -28] versus -23.5 [-29.5, -18.25]; P=0.046).

To analyze neuronal injury, infarct volume was quantified using TTC-staining brain sections collected at 24 and 72 hours after tMCAO. As shown in Figure 1J, there was significant reduction in infarct volume in SMS2$^{-/-}$ mice at 72 hours after tMCAO (Figure 1J; P=0.0021). However, there was no statistical significance between WT and SMS2$^{-/-}$ mice at 24 hours after tMCAO (Figure 1I; P=0.0502). Taken together, these results suggested that SMS2 deficiency played a protective role at 72 hours after cerebral I/R.

SMS2 Deficiency Suppressed the Overproduction of Inflammatory Mediators After Cerebral I/R

Inflammatory response mediated by the TLRs signaling pathway plays a critical role in ischemic stroke. Recent studies have demonstrated that Gal-3 is required for activation of the TLRs signaling pathway after cerebral ischemic injury.[28] As an endogenous ligand of TLR4, Gal-3 is considered as a novel inflammatory mediator during I/R. Therefore, we determined the expression of Gal-3 in brain tissues after cerebral I/R. In line with a previous study, the protein level of Gal-3 was significantly increased after tMCAO in a time-dependent manner with a maximum induction at 72 hours after tMCAO (Figure 2A; n=4; P<0.0001).[29] Importantly, mRNA and protein expression of Gal-3 triggered by tMCAO was dramatically decreased in SMS2$^{-/-}$ mice at 72 hours after tMCAO (Figure 2B; tMCAO: WT group versus SMS2$^{-/-}$ group: 1.26 [1.04, 1.65] versus 0.59 [0.51, 0.73] [protein level], 84.24 [82.51, 91.13] versus 48.90 [46.07, 62.08] [mRNA level], n=4; P=0.021).

We then analyzed the mRNA level of the key inflammatory mediators involved in cerebral I/R. Transcription of interleukin-1 beta, a proinflammatory cytokine, was suppressed in SMS2$^{-/-}$ mice at 72 hours after tMCAO (Figure 2D; tMCAO: WT group versus SMS2$^{-/-}$ group: 5.15 [4.43, 10.92] versus 1.38 [0.89, 2.52], n=4; P=0.027). In contrast, expression of Arg-1, taken as an M2 marker of microglia polarization and a well-known modulator of central nervous system injury, was significantly increased at both 24 and 72 hours after tMCAO (Figure 2C; n=4; P=0.043; Figure 2D; tMCAO: WT group versus SMS2$^{-/-}$ group: 109.71 [23, 272.27] versus 375.87 [226.33, 608.12] [72 hours], n=4; P=0.043). We also determined the mRNA levels of iNOS, which competes with Arg-1 in the consumption of arginine. There was no statistical significance in the expression of iNOS between WT and SMS2$^{-/-}$ mice, although a trend of reduced iNOS expression was observed in SMS2$^{-/-}$ mice after tMCAO (Figure 2C; n=4; P=0.386; Figure 2D; n=4; P=0.602). These data demonstrated that SMS2 deficiency exerted potent anti-inflammatory effects during cerebral I/R.

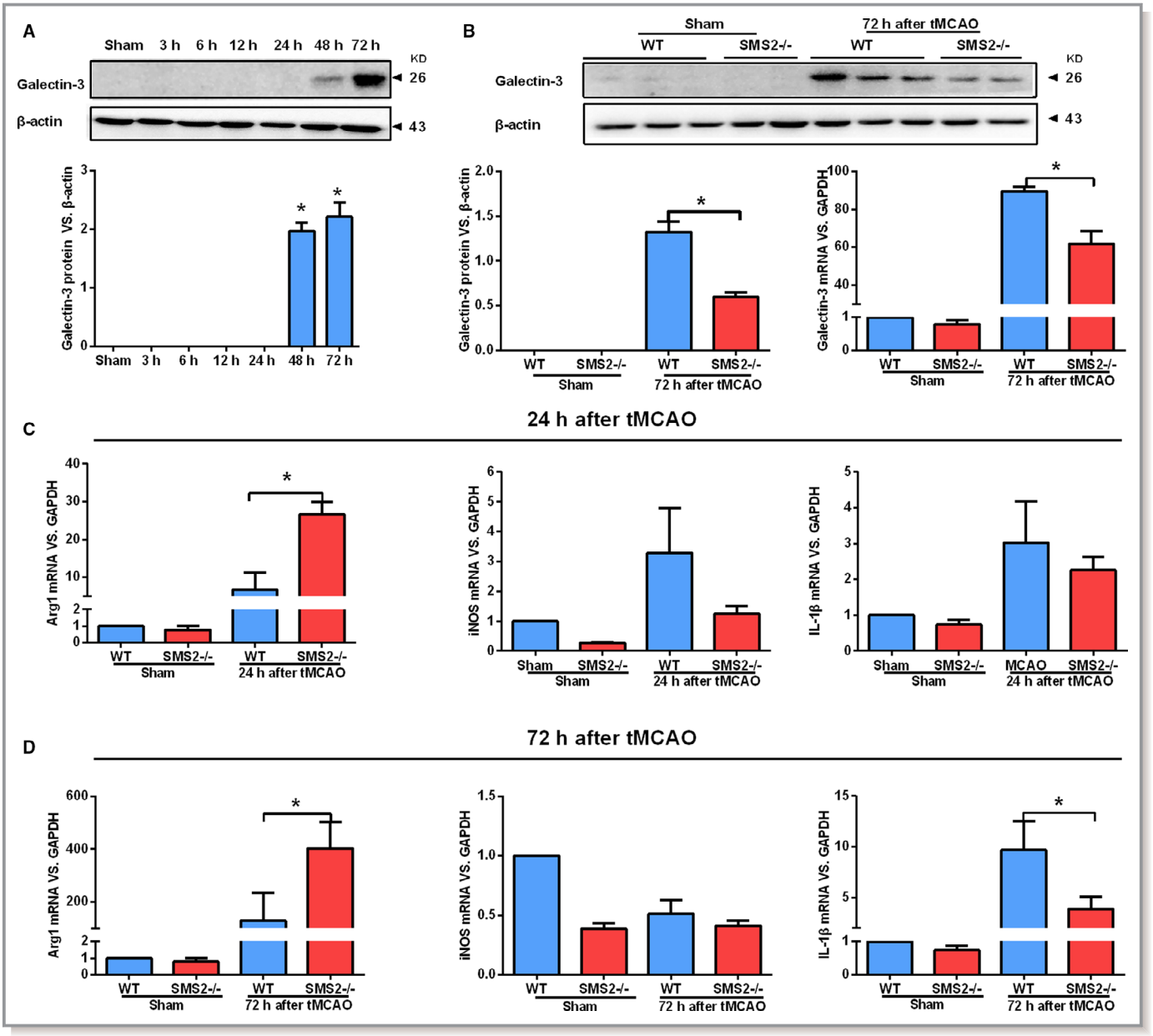

Figure 2. SMS2 knockout mice showed a decreased expression of inflammation-related mediators after cerebral ischemic reperfusion. **A**, Quantification of galectin-3 protein levels at indicated time points after cerebral ischemic reperfusion in the peri-infarct region of WT mice (*P<0.05 vs sham group, nonparametric Mann–Whitney U test). **B**, Quantification of galectin-3 protein and mRNA levels in WT and SMS2$^{-/-}$ mice at 72 hours after cerebral ischemic reperfusion in the peri-infarct region (*P<0.05 vs WT group, nonparametric Mann–Whitney U test). **C**, Quantification of mRNA levels of Arg-1, iNOS, and IL-1β in WT and SMS2$^{-/-}$ mice at 24 hours after cerebral ischemic reperfusion in the peri-infarct region. **D**, Quantification of mRNA levels of Arg-1, iNOS, and IL-1β in WT and SMS2$^{-/-}$ mice at 72 hours after cerebral ischemic reperfusion in the peri-infarct region (*P<0.05 vs WT group, nonparametric Mann–Whitney U test). Data are mean±SEM; n=4 for each group. Arg-1 indicates arginase 1; iNOS, inducible nitric oxide synthase; IL-1β, interleukin-1 beta; SMS2, sphingomyelin synthase 2; tMCAO, transient middle cerebral artery occlusion; WT, wild type.

SMS2 Deficiency Suppressed Microglia Activation After Cerebral I/R

Cerebral I/R is always accompanied with rapid microglial activation, leading to the inflammatory cascade reaction and secretion of proinflammatory cytokines. Recent studies have demonstrated that Gal-3 expression is predominantly produced and localized in activated microglia, indicating that Gal-3-positive microglia may represent proinflammatory M1 microglia.[30,31] We then performed immunofluorescence staining to examine the impact of SMS2 deficiency on Gal-3 expression in microglia (Figure 3A). The number of microglia (Iba-1^{+} cells) was comparable between SMS2$^{-/-}$ and WT mice at both 24 and

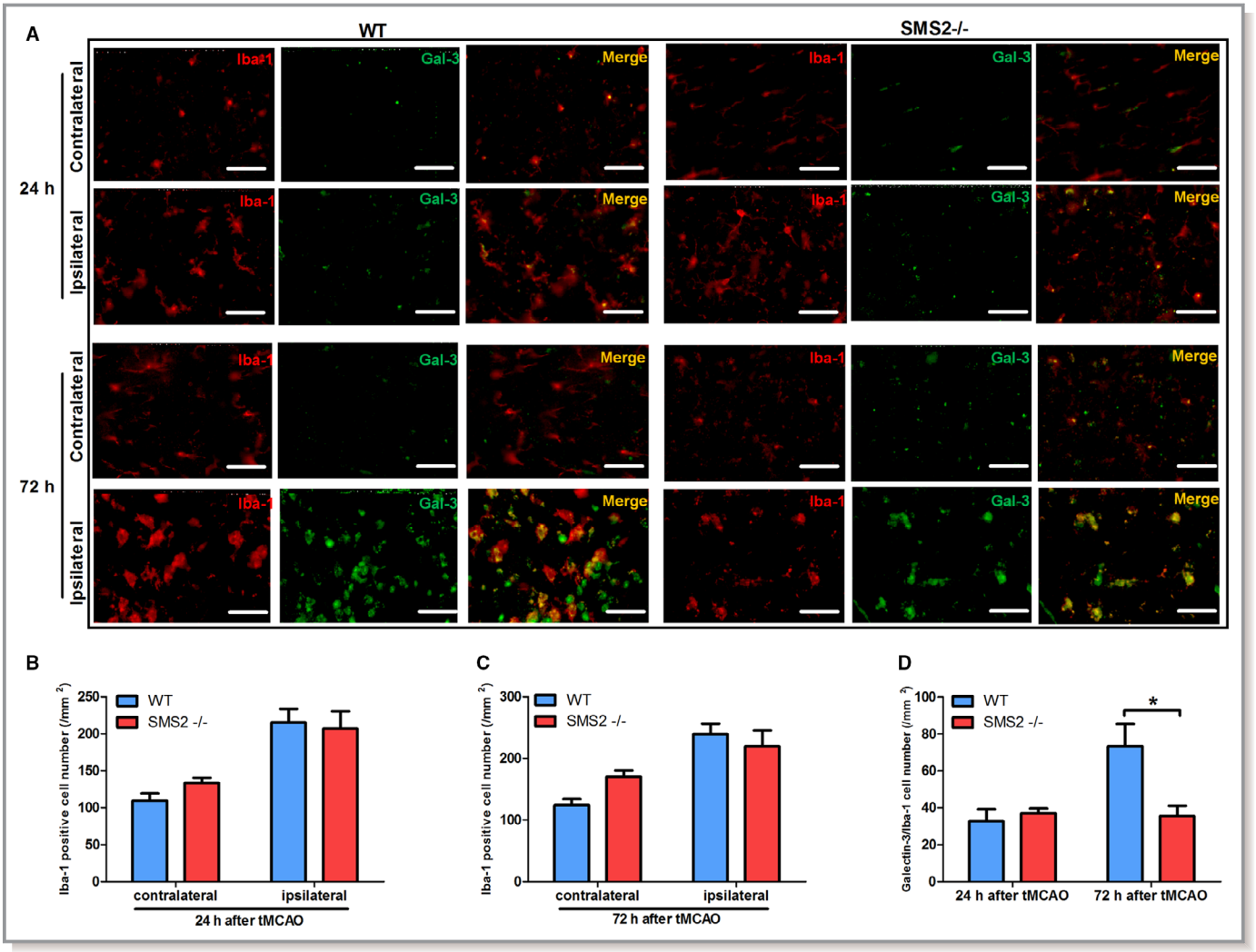

Figure 3. SMS2 deficiency inhibited the activation of microglia after cerebral ischemic reperfusion. **A**, Representative images of Iba-1^{+}/Gal-3^{+} cells in brains from the nonischemic hemisphere and ischemic hemisphere at 24 and 72 hours after cerebral ischemic reperfusion. Scale bar, 50 μm. **B** and **C**, Quantification of the numbers of Iba-1^{+} cells in WT and SMS2$^{-/-}$ mice at 24 and 72 hours after cerebral ischemic reperfusion. **D**, Quantification of the numbers of Iba-1^{+}Gal-3^{+} cells in WT and SMS2$^{-/-}$ mice at 72 hours after cerebral ischemic reperfusion (*P<0.05, 1-way ANOVA). Data are mean±SEM; n=4 for each group. Gal-3 indicates galectin-3; Iba-1, ionized calcium binding adaptor molecule-1; SMS2, sphingomyelin synthase 2; tMCAO, transient middle cerebral artery occlusion; WT, wild type.

72 hours after cerebral I/R (Figure 3B; n=4; P=0.0717; Figure 3C; n=4; P=0.425), indicating that lack of SMS2 did not affect microglia homeostasis. Notably, the number of Gal-3-producing microglia (Gal-3^{+}Iba-1^{+} cells) remarkably decreased in SMS2$^{-/-}$ mice at 72 hours after cerebral I/R (Figure 3D; n=4; P=0.000). These results suggested that SMS2 deficiency might inhibit microglia activation, and thus suppress Gal-3 production, subsequently attenuating the initiation of inflammatory response during cerebral I/R.

SMS2 Deficiency Attenuated the Activation of TLR4/NF-κB Signaling Pathway After Cerebral I/R

In several neurodegenerative diseases, activation of microglia occurs through the triggering of pathogen recognition receptors, such as TLR4.[32] Previously, SMS2 deficiency has been reported to inhibit NF-κB activation through the TLR4 signaling pathway in macrophage.[11] To clarify whether SMS2 deficiency suppressed microglia activation through the TLR4/NF-κB pathway, we first examined the translocation of NF-κB at 24 and 72 hours after cerebral I/R (Figure 4A and 4C). As we expected, the translocation of the NF-κB–p65 subunit into the nucleus was significantly halted in SMS2$^{-/-}$ mice compared with WT mice at both 24 and 72 hours after cerebral I/R (Figure 4B; tMCAO: WT group versus SMS2$^{-/-}$ group: 1.20 [1.13, 1.85] versus 0.93 [0.78, 1.19] [nuclear], 0.57 [0.45, 0.66] versus 1.33 [1.18, 1.89] [plasma], n=4; P=0.043 and 0.004, respectively; Figure 4D; 1.95 [1.66, 2.43] versus 1.52 [0.39, 1.85] [nuclear], 0.87 [0.67, 1.83] versus 2.46 [1.81, 3.24] [plasma], n=4; P=0.033 and 0.016, respectively).

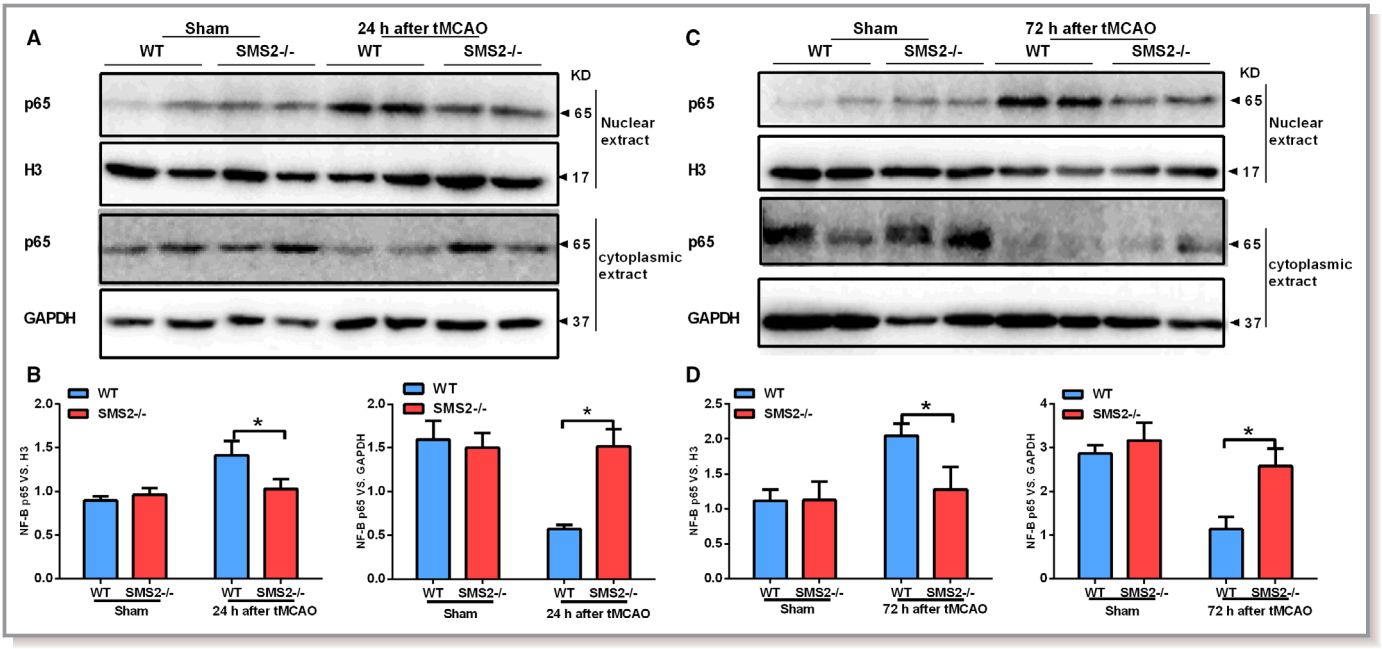

Figure 4. SMS2 deficiency led to a decreased nuclear translocation of NF-κB after cerebral ischemic reperfusion. **A** and **B**, Representative images and quantification of NF-κB p65 protein levels in nuclear and cytoplasmic at 24 hours after cerebral ischemic reperfusion in peri-infarct region of WT and SMS2$^{-/-}$ mice (*P<0.05 vs WT group, nonparametric Mann–Whitney U test). **C** and **D**, Representative images and quantification of NF-κB p65 protein levels in nuclear and cytoplasmic at 72 hours after cerebral ischemic reperfusion in the peri-infarct region of WT and SMS2$^{-/-}$ mice (*P<0.05 vs WT group, nonparametric Mann–Whitney U test). Data are mean±SEM; n=4. NF-κB indicates nuclear factor kappa-light-chain-enhancer of activated B cells; SMS2, sphingomyelin synthase 2; WT, wild type.

SMS2 Deficiency Impaired the Recruitment of TLR4 to Lipid Raft Both In Vivo and In Vitro

We then assessed the recruitment of TLR4 and its coreceptor, MD2, on the cell surface of microglia at 72 hours after tMCAO by flow cytometry. In the current experiment, microglia could be identified as CD11b^{+}/CD45^{int} cells in brain tissues (Figure 5A).[13] Flow cytometry analysis showed that there was no significant difference in the surface expression of TLR4 between the WT and SMS2$^{-/-}$ groups (data not shown). However, reduced levels of the TLR4/MD2 complex on the microglia surface were observed in SMS2$^{-/-}$ mice compared with WT mice after cerebral I/R, which is consistent with a previous report[11] (Figure 5B; n=4; P=0.007).

Membrane lipid rafts are involved with TLR4 signaling, given that recruitment of TLR4 to lipid rafts is essential for the formation of the TLR4/MD2 complex and downstream signaling cascades.[33] Moreover, a previous study has demonstrated that SMS2 deficiency could interrupt TLR4 recruitment to lipid rafts after LPS stimulation in macrophages.[34] Thus, we hypothesized that SMS2 deficiency could interrupt TLR4 recruitment to lipid rafts after cerebral I/R. To test this hypothesis, we isolated lipid rafts from brain tissue after cerebral I/R and analyzed the top 12 fractions to substantiate lipid raft localization of TLR4. Our results showed that recruitment of TLR4 into lipid rafts (fraction, 4–6) was decreased in SMS2$^{-/-}$ mice compared with WT mice after cerebral I/R (Figure 5C). The level of flotillin-1, a canonical marker of lipid rafts, was comparable between WT and SMS2$^{-/-}$ mice.

To ascertain the involvement of SMS2 on the trafficking of TLR4 to lipid rafts, we conducted experiments in a microglia cell line (BV2 cells). BV2 cells were pretreated with a competitive inhibitor of SMS, D609, for 2 hours, followed by incubation with LPS, an exogenous ligand of TLR4. Cells treated with LPS either in the presence or absence of D609 were stained with anti-TLR4/MD2 antibody. As shown in Figure 5D, cellular stimulation with LPS induced the formation of TLR4/MD2, whereas the complex formation was significantly inhibited by D609 treatment (Figure 5D; P=0.000).

SMS2 Deficiency Impaired the Recruitment of TLR4 to Lipid Rafts by Altering the Level of Sphingomyelin in Lipid Raft Fractions

SMS2 is a rate-limiting enzyme for the synthesis of sphingomyelin, which is a major component of lipid rafts and plays a pivotal role in the function of the intact lipid raft.[34] We hypothesized that SMS2 deficiency may regulate the recruitment of TLR4 to lipid rafts by reducing sphingomyelin levels in lipid raft fractions and thus reducing the formation of the TLR4/MD2 complex after cerebral I/R. To determine the

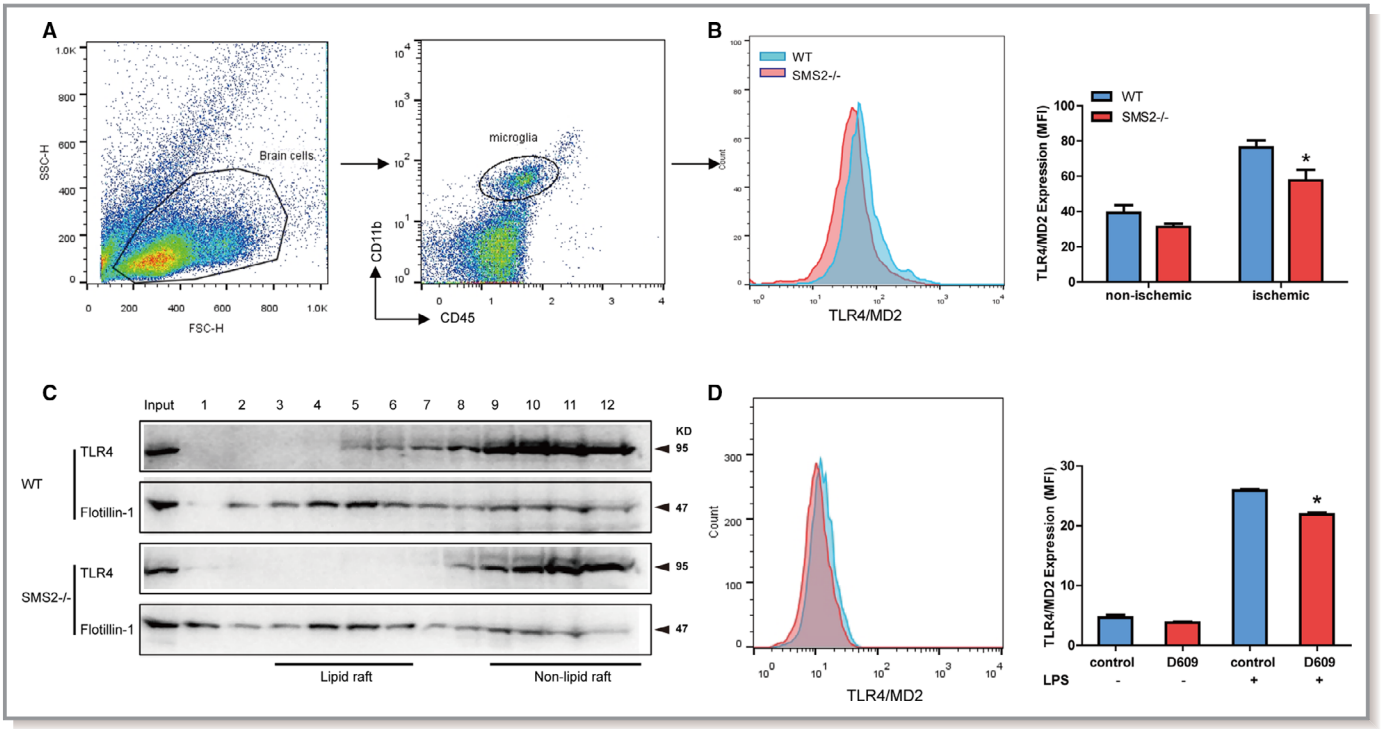

Figure 5. SMS2 deficiency decreased the level of TLR4/MD2 on the cell surface of microglia and reduced the recruitment of TLR4 into lipid rafts after cerebral ischemic reperfusion. **A** and **B**, Microglia isolated from brains of the nonischemic hemisphere and ischemic hemisphere in WT and SMS2$^{-/-}$ mice were stained with TLR4/MD2 complex antibody and analyzed on a flow cytometer. Results shown are a representative of 3 independent experiments (*P<0.05, 1-way ANOVA). Data are mean±SEM; n=4. **C**, Effects of SMS2 deficiency on brain TLR4 recruitment to lipid rafts in mouse brain after cerebral ischemic reperfusion. The panel shows TLR4 and flotillin-1 expression in each fraction in the peri-infarct region. **D**, BV2 cells were pretreated with vehicle or D609 (100 μmol/L) for 2 hours and then were treated with LPS (200 ng/mL) for 30 minutes. TLR4/MD2 expression was analyzed by flow cytometry (*P<0.05; 1-way ANOVA). Results shown are a representative of 3 independent experiments. FSC indicates forward scatter; MFI, mean fluorescence intensity; SSC, side scatter; SMS2, sphingomyelin synthase 2; TLR4/MD2, Toll-like receptor 4/myeloid differentiation factor 2; WT, wild type.

impact of SMS2 deficiency on brain sphingomyelin level, sphingomyelin levels were measured with liquid chromatography/electrospray ionization/tandem mass spectrometry. Using liquid chromatography/electrospray ionization/tandem mass spectrometry, we demonstrated that the SMS2$^{-/-}$ group had a significantly reduced level of C16-sphingomyelin, C18:1-sphingomyelin, C18-sphingomyelin, C20:1-sphingomyelin, C22:1-sphingomyelin, C22-sphingomyelin, C24:1-sphingomyelin, and C24-sphingomyelin at sham, 12, 24, and 72 hours after cerebral I/R (Figure 6A through 6D), indicating that SMS2 deficiency dramatically reduced sphingomyelin levels of brain.

We then compared the level of sphingomyelin in the lipid raft factions and non-lipid-raft fractions between WT and SMS2$^{-/-}$ mice. The results showed that a significantly reduced level of sphingomyelin, such as C16-sphingomyelin, C18:1-sphingomyelin, and C18-sphingomyelin, were detected in the fractions of brain lipid raft in SMS2$^{-/-}$ mice (Figure 6E; lipid rafts: WT group versus SMS2$^{-/-}$ group: 10 292.70 [7424.84, 13 695.65] versus 5857.90 [4400, 7226.28]; P=0.031; Figure 6F; 149 129.35 [86 339.87, 177 131.80] versus 63 853.08 [41 875, 79 929.58]; P=0.01; Figure 6G; 7959.60 [4519.58, 9697.00] versus 3010.46 [673.98, 4403.33]; P=0.012). These findings uniformly suggested that SMS2 deficiency that impaired the recruitment of TLR4 into lipid raft may attributed, at least partly, to altering the sphingomyelin level in lipid raft fractions.

Discussion

In the present study, we demonstrate, for the first time, that: (1) SMS2 deficiency led to beneficial outcomes after cerebral I/R in mice; (2) SMS2 deficiency reduced the number of activated microglia after cerebral I/R; (3) the production of key proinflammatory mediators were dramatically decreased in SMS2$^{-/-}$ mice after cerebral I/R; (4) NF-κB activation was attenuated in SMS2$^{-/-}$ mice; (5) TLR4 activation and TLR4/MD2 complex formation were repressed in SMS2$^{-/-}$ mice; and (6) SMS2 deficiency–induced low sphingomyelin levels in lipid rafts, may be compromising TLR4/MD2 complex formation.

Emerging evidence suggests that postischemic inflammation plays an important role in determining the outcome of

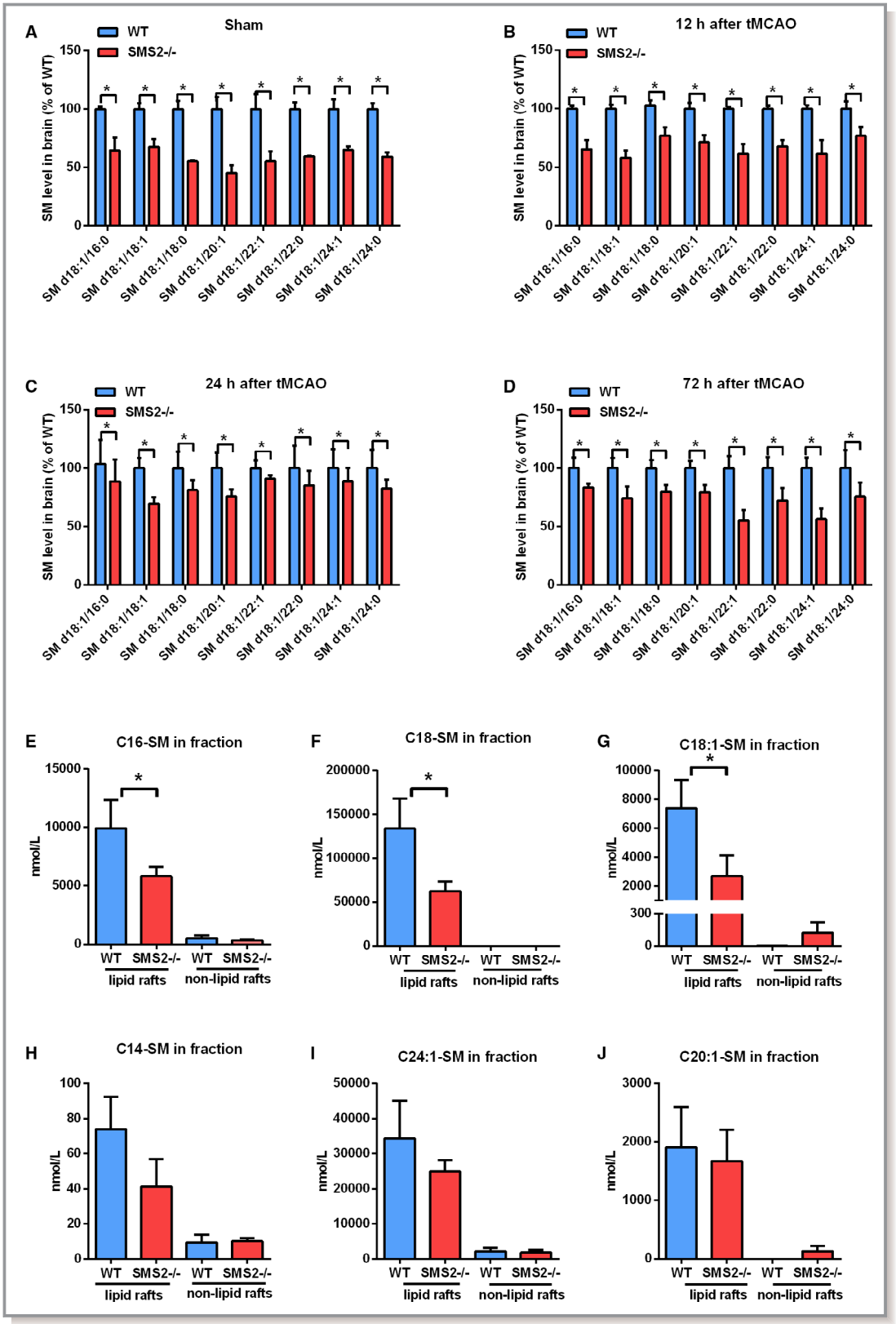

Figure 6. SMS2 deficiency led to a decreased sphingomyelin level. **A** through **D**, Brain sphingomyelin levels of WT mice and SMS2$^{-/-}$ mice at 0, 12, 24, and 72 hours after cerebral ischemic reperfusion (n=4). **E** through **J**, Levels of sphingomyelin in lipid rafts and nonlipid rafts fractions isolated from WT and SMS2$^{-/-}$ mice brain (*P<0.05 vs WT group, Mann–Whitney U test). Data are mean±SEM; n=4. SM indicates sphingomyelin; SMS2, sphingomyelin synthase 2; tMCAO, transient middle cerebral artery occlusion; WT, wild type.

ischemic stroke.[35] In clinical practice, increased production of proinflammatory cytokines is related to expanded volumes of infarct region and detrimental consequences in patients suffering from ischemic stroke.[36] We and others have previously demonstrated that cerebral I/R could result in an inflammatory process.[37,38] Therefore, reducing inflammation emerges as a therapeutic opportunity for improving functional outcomes after cerebral I/R.

Given that neurological scores and gait analyses have been widely applied in clinical practice for assessing the severity of ischemic stroke, in the current study, we evaluated the neurological function of mice by neurological scores, gait analyses, and sensorimotor tests, such as the corner test. We found that the 28-point neuroscore, neurological scores, corner test, and gait parameters were affected in mice subjected to tMCAO, which is partially in line with other studies.[15,16,18] Importantly, our results showed that SMS2$^{-/-}$ mice subjected to tMCAO had less-severe brain injury than WT mice, as indicated by improved neurological function and reduced infarct volume at 72 hours after tMCAO. The improvement of neurological functions and infarct volume has been considered to be connected with the reduction of postischemic inflammation.[39] Considering the anti-inflammatory effect of SMS2 deficiency, it could be concluded that the neuroprotective effect of SMS2 deficiency could be mediated by its anti-inflammatory activity.

As the resident macrophages of the central nervous system, microglia are responsible for the inflammation after cerebral I/R through secreting proinflammatory cytokine, such as interleukin-1 beta. Microglia could be driven to adopt M1 and M2 phenotypes, with iNOS as the classical M1 marker and Arg-1 as the M2 marker.[40] Our current results showed that SMS2 deficiency exhibited decreased expression of interleukin-1 beta and increased expression of Arg-1. However, there was no difference in the number of Iba-1^{+} microglia between WT and SMS2$^{-/-}$ mice. Collectively, these results suggested that SMS2 deficiency might modulate microglia activation other than influencing the microglia population to ameliorate inflammatory responses caused by cerebral I/R.

Microglia can be activated through many signaling pathways, especially TLR4 signal-transduction cascade.[32] Activation of the TLR4 signaling pathway is triggered by the binding of exogenous or endogenous ligands to the extracellular domain of TLR4.[28] In the peri-infarct region, activated microglia express high levels of Gal-3, a β-galactoside–binding lectin, which has been identified as an endogenous ligand of TLR4 and plays an important role in initiating downstream inflammatory responses.[28,30] Recent studies have demonstrated that Gal-3 is attributed to the activation of microglia and is required for proper induction of TLR response after ischemic injury. Therefore, Gal-3 may be involved in the process of postischemic inflammation, microglia activation, and cytokine secretion at the beginning stage after stroke. In our results, SMS2 deficiency significantly reduced the expression of Gal-3 and Gal-3-producing microglia (Gal-3^{+}Iba-1^{+} cells) after cerebral I/R. Moreover, SMS2$^{-/-}$ mice displayed less severe brain injury than WT mice at 72 hours after tMCAO. We speculated that SMS2 deficiency could inhibit microglia activation at first, then released less of a level of Gal-3, which further inhibited the TLR4 pathway to exert anti-inflammatory and neuroprotective effects. To further understand the mechanisms underlying the anti-inflammatory effect of SMS2 deficiency, we investigated the role of SMS2 deficiency on the TLR4 signaling pathway in cerebral I/R.

Accumulated evidence has demonstrated that TLR4/NF-κB signaling mediates microglia activation and postischemic inflammation after cerebral I/R.[41,42] In the present study, our data demonstrated that SMS2 deficiency blocked nuclear translocation of NF-κB and reduced the overproduction of downstream inflammatory cytokines after cerebral I/R. Our conclusion is supported by previous findings that SMS2 deficiency suppressed LPS-induced inflammation in macrophages through the TLR4/NF-κB pathway.[11] During the process of TLR4 signaling pathway activation, recruitment of TLR4 into lipid rafts is the first step, leading to the formation of the TLR4/MD2 complex to activate downstream signal transduction.[43] Lipid rafts are membrane microdomains enriched in cholesterol, sphingolipid, and glycolipid. It has been proposed as platforms for promoting the interaction of protein complex, such as the TLR4/MD2 complex, and modulating signal transduction.[44] Several studies have suggested an important role for lipid rafts in the TLR4 signaling pathway. Methyl-β-cyclodextrin, a raft-disrupting agent, has been shown to be capable of inhibiting the TLR4 signaling pathway and reducing proinflammatory cytokine production.[45] Previous studies have demonstrated that I/R induced the recruitment of TLR4 to lipid raft.[5] Because SMS2 plays a crucial role in the correct function of lipid rafts through mediating sphingomyelin biosynthesis, we reasoned that SMS2 deficiency might have an impact on TLR4 translocation to lipid rafts after cerebral I/R. Indeed, coupled with the data obtained by flow cytometry and immunofluorescence microscopy, we demonstrated that SMS2 deficiency decreased the expression of the TLR4/MD2 complex in microglia and inhibited recruitment of TLR4 into lipid raft fractions after cerebral I/R. This observation is consistent with Hailemariam et al that SMS2 deficiency diminished the abundance of TLR4/MD2 complex on the surface of macrophages after LPS stimulation.[11] A similar effect was observed when SMS2 was inhibited pharmacologically with the inhibitor, D609. These results indicated that SMS2 deficiency suppressed the TLR4/NF-κB signaling pathway by impeding TLR4 trafficking to lipid rafts.

The connection between neurological disease and disrupted lipid homeostasis has been reflected in the alterations of lipid raft components.[8] As 1 of the major components of lipid rafts, sphingomyelin level is critical to maintain the function of lipid rafts. As a rate-limiting synthetic enzyme of sphingomyelin, SMS2 has biological roles in regulating membrane fluidity and the structure of lipid rafts. Previous studies have demonstrated that SMS2 deficiency could regulate LPS-TLR4–induced inflammatory responses by remodeling the structure of lipid rafts.[11] Consistent with previous studies, we demonstrated that SMS2$^{-/-}$ mice brain had significantly reduced level of sphingomyelin. In addition, our results showed that sphingomyelin levels of lipid raft fractions were significantly decreased in SMS2$^{-/-}$ mice. These results suggested that SMS2 deficiency might interfere with TLR4 recruitment by altering sphingomyelin components during cerebral I/R.

In summary, SMS2 deficiency exerted an anti-inflammatory effect in cerebral I/R by alleviating TLR4 recruitment to lipid rafts and suppressing its downstream signal transduction. These findings may shed light on a therapeutic design focusing on the disturbance of membrane component homeostasis to subsequently restrict the inflammatory signaling pathways.

Sources of Funding

This work was funded by the National Natural Science Foundation of China (81371287, Dr X. Zhang; 81571292, Dr X. Zhang; 91539114, Dr Qin; and 81141046, Dr Yu) and the Taishan Scholars Program of Shandong Province (ts201511057 to Dr Qin; tsqn20161045 to Song).

Disclosures

None.

References

1. Jin R, Yang G, Li G. Inflammatory mechanisms in ischemic stroke: role of inflammatory cells. *J Leukoc Biol*. 2010;87:779–789.
2. Hacke W, Kaste M, Bluhmki E, Brozman M, Davalos A, Guidetti D, Larrue V, Lees KR, Medeghri Z, Machnig T, Schneider D, von Kummer R, Wahlgren N, Toni D; ECASS Investigators. Thrombolysis with alteplase 3 to 4.5 hours after acute ischemic stroke. *N Engl J Med*. 2008;359:1317–1329.
3. Brea D, Blanco M, Ramos-Cabrer P, Moldes O, Arias S, Perez-Mato M, Leira R, Sobrino T, Castillo J. Toll-like receptors 2 and 4 in ischemic stroke: outcome and therapeutic values. *J Cereb Blood Flow Metab*. 2011;31:1424–1431.
4. Caso JR, Pradillo JM, Hurtado O, Leza JC, Moro MA, Lizasoain I. Toll-like receptor 4 is involved in subacute stress-induced neuroinflammation and in the worsening of experimental stroke. *Stroke*. 2008;39:1314–1320.
5. Powers KA, Szaszi K, Khadaroo RG, Tawadros PS, Marshall JC, Kapus A, Rotstein OD. Oxidative stress generated by hemorrhagic shock recruits Toll-like receptor 4 to the plasma membrane in macrophages. *J Exp Med*. 2006;203:1951–1961.
6. Simons K, Toomre D. Lipid rafts and signal transduction. *Nat Rev Mol Cell Biol*. 2000;1:31–39.
7. Olsson S, Sundler R. The role of lipid rafts in LPS-induced signaling in a macrophage cell line. *Mol Immunol*. 2006;43:607–612.
8. Sonnino S, Aureli M, Grassi S, Mauri L, Prioni S, Prinetti A. Lipid rafts in neurodegeneration and neuroprotection. *Mol Neurobiol*. 2014;50:130–148.
9. Liu J, Huan C, Chakraborty M, Zhang H, Lu D, Kuo MS, Cao G, Jiang XC. Macrophage sphingomyelin synthase 2 deficiency decreases atherosclerosis in mice. *Circ Res*. 2009;105:295–303.
10. Kidani Y, Ohshima K-ı, Sakai H, Kohno T, Baba A, Hattori M. Differential localization of sphingomyelin synthase isoforms in neurons regulates sphingomyelin cluster formation. *Biochem Biophys Res Commun*. 2012;417:1014–1017.
11. Hailemariam TK, Huan C, Liu J, Li Z, Roman C, Kalbfeisch M, Bui HH, Peake DA, Kuo MS, Cao G, Wadgaonkar R, Jiang XC. Sphingomyelin synthase 2 deficiency attenuates NFκB activation. *Arterioscler Thromb Vasc Biol*. 2008;28:1519–1526.
12. Xue J, Zhang X, Zhang C, Kang N, Liu X, Yu J, Zhang N, Wang H, Zhang L, Chen R, Cui L, Wang L, Wang X. Protective effect of Naoxintong against cerebral ischemia reperfusion injury in mice. *J Ethnopharmacol*. 2016;182:181–189.
13. Clarkson BDS, Ling C, Shi Y, Harris MG, Rayasam A, Sun D, Salamat MS, Kuchroo V, Lambris JD, Sandor M, Fabry Z. T cell–derived interleukin (IL)-21 promotes brain injury following stroke in mice. *J Exp Med*. 2014;211:595–604.
14. Yang G, Chan PH, Chen J, Carlson E, Chen SF, Weinstein P, Epstein CJ, Kamii H. Human copper-zinc superoxide dismutase transgenic mice are highly resistant to reperfusion injury after focal cerebral ischemia. *Stroke*. 1994;25:165–170.
15. Encarnacion A, Horie N, Keren-Gill H, Bliss TM, Steinberg GK, Shamloo M. Long-term behavioral assessment of function in an experimental model for ischemic stroke. *J Neurosci Methods*. 2011;196:247–257.
16. Kishida N, Maki T, Takagi Y, Yasuda K, Kinoshita H, Ayaki T, Noro T, Kinoshita Y, Ono Y, Kataoka H, Yoshida K, Lo EH, Arai K, Miyamoto S, Takahashi R. Role of perivascular oligodendrocyte precursor cells in angiogenesis after brain ischemia. *J Am Heart Assoc*. 2019;8:e011824. DOI: 10.1161/JAHA.118.011824.
17. Weise G, Posel C, Moller K, Kranz A, Didwischus N, Boltze J, Wagner DC. High-dosage granulocyte colony stimulating factor treatment alters monocyte trafficking to the brain after experimental stroke. *Brain Behav Immun*. 2017;60:15–26.
18. Tatlisumak T, Carano RA, Takano K, Opgenorth TJ, Sotak CH, Fisher M. A novel endothelin antagonist, A-127722, attenuates ischemic lesion size in rats with temporary middle cerebral artery occlusion: a diffusion and perfusion MRI study. *Stroke*. 1998;29:850–857; discussion 857–858.
19. Yu Y, Cui Y, Zhao Y, Liu S, Song G, Jiao P, Li B, Luo T, Guo S, Zhang X, Wang H, Jiang XC, Qin S. The binding capability of plasma phospholipid transfer protein, but not HDL pool size, is critical to repress LPS induced inflammation. *Sci Rep*. 2016;6:20845.
20. Zhao J, Zhang X, Dong L, Wen Y, Zheng X, Zhang C, Chen R, Zhang Y, Li Y, He T, Zhu X, Li L. Cinnamaldehyde inhibits inflammation and brain damage in a mouse model of permanent cerebral ischaemia. *Br J Pharmacol*. 2015;172:5009–5023.
21. Sierra A, Gottfried-Blackmore AC, McEwen BS, Bulloch K. Microglia derived from aging mice exhibit an altered inflammatory profile. *Glia*. 2007;55:412–424.
22. He H, Geng T, Chen P, Wang M, Hu J, Kang L, Song W, Tang H. NK cells promote neutrophil recruitment in the brain during sepsis-induced neuroinflammation. *Sci Rep*. 2016;6:27711.
23. Persaud-Sawin DA, Lightcap S, Harry GJ. Isolation of rafts from mouse brain tissue by a detergent-free method. *J Lipid Res*. 2008;50:759–767.
24. Zhang Y, Chen F, Chen J, Huang S, Chen J, Huang J, Li N, Sun S, Chu X, Zha L. Soyasaponin Bb inhibits the recruitment of Toll-like receptor 4 (TLR4) into lipid rafts and its signaling pathway by suppressing the nicotinamide adenine dinucleotide phosphate (NADPH) oxidase-dependent generation of reactive oxygen species. *Mol Nutr Food Res*. 2016;60:1532–1543.
25. Peng B, Weintraub ST, Coman C, Ponnaiyan S, Sharma R, Tews B, Winter D, Ahrends R. A comprehensive high-resolution targeted workflow for the deep profiling of sphingolipids. *Anal Chem*. 2017;89:12480–12487.
26. Zhao YY, Xiong Y, Curtis JM. Measurement of phospholipids by hydrophilic interaction liquid chromatography coupled to tandem mass spectrometry: the determination of choline containing compounds in foods. *J Chromatogr A*. 2011;1218:5470–5479.
27. Bouet V, Freret T, Toutain J, Divoux D, Boulouard M, Schumann-Bard P. Sensorimotor and cognitive deficits after transient middle cerebral artery occlusion in the mouse. *Exp Neurol*. 2007;203:555–567.
28. Burguillos Miguel A, Svensson M, Schulte T, Boza-Serrano A, Garcia-Quintanilla A, Kavanagh E, Santiago M, Viceconte N, Oliva-Martin Maria J, Osman Ahmed M, Salomonsson E, Amar L, Persson A, Blomgren K, Achour A, Englund E,

Leffler H, Venero Jose L, Joseph B, Deierborg T. Microglia-secreted galectin-3 acts as a Toll-like receptor 4 ligand and contributes to microglial activation. *Cell Rep*. 2015;10:1626–1638.

29. Walther M, Kuklinski S, Pesheva P, Guntinas-Lichius O, Angelov DN, Neiss WF, Asou H, Probstmeier R. Galectin-3 is upregulated in microglial cells in response to ischemic brain lesions, but not to facial nerve axotomy. *J Neurosci Res*. 2000;61:430–435.
30. Yang M, Kim J, Kim T, Kim SH, Kim JC, Kim J, Takayama C, Hayashi A, Joo HG, Shin T, Moon C. Possible involvement of galectin-3 in microglial activation in the hippocampus with trimethyltin treatment. *Neurochem Int*. 2012;61:955–962.
31. Lalancette-Hebert M, Swarup V, Beaulieu JM, Bohacek I, Abdelhamid E, Weng YC, Sato S, Kriz J. Galectin-3 is required for resident microglia activation and proliferation in response to ischemic injury. *J Neurosci*. 2012;32:10383–10395.
32. Heneka MT, Kummer MP, Latz E. Innate immune activation in neurodegenerative disease. *Nat Rev Immunol*. 2014;14:463–477.
33. Gianfrancesco MA, Paquot N, Piette J, Legrand-Poels S. Lipid bilayer stress in obesity-linked inflammatory and metabolic disorders. *Biochem Pharmacol*. 2018;153:168–183.
34. Filippov A, Oradd G, Lindblom G. Sphingomyelin structure influences the lateral diffusion and raft formation in lipid bilayers. *Biophys J*. 2006;90:2086–2092.
35. del Zoppo G, Ginis I, Hallenbeck JM, Iadecola C, Wang X, Feuerstein GZ. Inflammation and stroke: putative role for cytokines, adhesion molecules and iNOS in brain response to ischemia. *Brain Pathol*. 2000;10:95–112.
36. Vila N, Castillo J, Davalos A, Chamorro A. Proinflammatory cytokines and early neurological worsening in ischemic stroke. *Stroke*. 2000;31:2325–2329.
37. Marsh BJ, Stevens SL, Hunter B, Stenzel-Poore MP. Inflammation and the emerging role of the Toll-like receptor system in acute brain ischemia. *Stroke*. 2009;40:S34–S37.
38. Wen Y, Zhang X, Dong L, Zhao J, Zhang C, Zhu C. Acetylbritannilactone modulates microRNA-155-mediated inflammatory response in ischemic cerebral tissues. *Mol Med*. 2015;21:197–209.
39. Domin H, Przykaza L, Jantas D, Kozniewska E, Boguszewski PM, Smialowska M. Neuropeptide Y Y2 and Y5 receptors as promising targets for neuroprotection in primary neurons exposed to oxygen-glucose deprivation and in transient focal cerebral ischemia in rats. *Neuroscience*. 2017;344:305–325.
40. Lisi L, Ciotti GM, Braun D, Kalinin S, Curro D, Dello Russo C, Coli A, Mangiola A, Anile C, Feinstein DL, Navarra P. Expression of iNOS, CD163 and ARG-1 taken as M1 and M2 markers of microglial polarization in human glioblastoma and the surrounding normal parenchyma. *Neurosci Lett*. 2017;645:106–112.
41. Sun X, Zeng H, Wang Q, Yu Q, Wu J, Feng Y, Deng P, Zhang H. Glycyrrhizin ameliorates inflammatory pain by inhibiting microglial activation-mediated inflammatory response via blockage of the HMGB1-TLR4-NF-kB pathway. *Exp Cell Res*. 2018;369:112–119.
42. Wang L, Zhang X, Liu L, Cui L, Yang R, Li M, Du W. Tanshinone II A down-regulates HMGB1, RAGE, TLR4, NF-kappaB expression, ameliorates BBB permeability and endothelial cell function, and protects rat brains against focal ischemia. *Brain Res*. 2010;1321:143–151.
43. Fu Y, Zhou E, Wei Z, Wang W, Wang T, Yang Z, Zhang N. Cyanidin-3-O-beta-glucoside ameliorates lipopolysaccharide-induced acute lung injury by reducing TLR4 recruitment into lipid rafts. *Biochem Pharmacol*. 2014;90:126–134.
44. Allen JA, Halverson-Tamboli RA, Rasenick MM. Lipid raft microdomains and neurotransmitter signalling. *Nat Rev Neurosci*. 2007;8:128–140.
45. Regel G, Grotz M, Weltner T, Sturm JA, Tscherne H. Pattern of organ failure following severe trauma. *World J Surg*. 1996;20:422–429.